

# RGMA and neogenin protein expression are influenced by lens injury following optic nerve crush in the rat retina

Sven Schnichels · Peter Heiduschka · Sylvie Julien

Received: 23 May 2011 / Revised: 14 July 2011 / Accepted: 28 July 2011 / Published online: 2 September 2011  
© Springer-Verlag 2011

## Abstract

**Background** The death and the failure of neurons to regenerate their axons after lesion of the central nervous system in mammals, as in the case of spinal cord injury and optic nerve trauma, remain a challenge. In this study, we focused on the repulsive guidance molecule A (RGMA) and its receptor neogenin. Since it was reported that RGMA<sup>+</sup> cells accumulate in lesioned areas after spinal cord injury, brain trauma, and optic nerve crush, and curiously, anti-apoptotic effects of RGMA were also described, we investigated the role of RGMA and neogenin in the retina after optic nerve crush (ONC).

**Methods** We evaluated the spatial and temporal protein pattern of RGMA and neogenin in the rat retina without (non-regenerating model) or with (regenerating model) lens injury (LI). We investigated the presence of RGMA, neogenin and other proteins at up to nine time points

(6 h–20 days post-surgery) by performing immunohistochemistry and Western blots.

**Results** Independent of the treatment, RGMA protein was present in the nuclear layers (NLs), plexiform layers (PLs), nerve fiber layer (NFL), and in retinal ganglion cells (RGCs) of the rat retina. RGC and nerve fibers were always RGMA<sup>+</sup>. Further RGMA<sup>+</sup> cells in the retina were blood vessel endothelial cells, astrocytes, Müller cells, and some microglial cells. The RGMA pattern for the specific retinal cells resembled those of previously published data. The neogenin pattern was congruent to the RGMA pattern. Western blots of retinal tissue showed further RGMA<sup>+</sup> products only in LI animals. Furthermore, a higher amount of RGMA was found in the retinae of ONC + LI rats compared to ONC rats.

**Conclusions** Although a difference in the localization of RGMA is not obvious, the difference in the amount of RGMA is striking, the higher amount of RGMA in the retinae of ONC + LI rats compared to ONC rats indicates a role for RGMA during degeneration/regeneration processes. Our results are consistent with several reported neuro-protective effects of RGMA. Our new data showing the upregulation of RGMA after ONC in our regenerating model (plus LI) confirm these findings conducted in different settings.

**Electronic supplementary material** The online version of this article (doi:10.1007/s00417-011-1791-9) contains supplementary material, which is available to authorized users.

S. Schnichels  
Centre for Ophthalmology, University Eye Hospital,  
Tübingen, Germany

P. Heiduschka · S. Julien (✉)  
Section for Experimental Vitreoretinal Surgery,  
Centre for Ophthalmology, Institute for Ophthalmic Research,  
Schleichstr. 12/1,  
72076 Tübingen, Germany  
e-mail: sylvie.julien@med.uni-tuebingen.de

## Present Address:

P. Heiduschka  
University Eye Hospital,  
Domagkstr. 15,  
48149 Münster, Germany

**Keywords** RGMA · Neogenin · Optic nerve crush · Retina · Lens injury · Retinal ganglion cells · Regeneration

## Introduction

In-vivo, neurons of the central nervous system (CNS) lack the ability to regenerate their axons after an injury. After optic nerve trauma in adult rats, a rapid and massive

reduction of the original population of retinal ganglion cells (RGC) is observed, starting 5–7 days after injury. Some 80% to more than 90% of the RGCs die within 2 weeks after the injury [1–8]. RGC loss is slower in crushed than in transected optic nerves [6, 9]. The reasons for the failure of RGC axons to regenerate after optic nerve lesions in adult animals are not known. Plausible hypotheses include down-regulation of cytoskeletal proteins, receptors, or proteins involved in the signaling pathways necessary for axonal elongation [10] and/or expression of receptors for molecules inhibitory to axonal extension, such as NOGO, netrin-1, semaphorins, and ephrins [11–16].

A further chemorepulsive factor playing a role in CNS disorders is the Repulsive Guidance Molecule (RGM), which has been functionally characterized as a molecular determinant for retinotectal map formation [17–19]. RGM is attached to membranes via a glycosylphosphatidylinositol (GPI) anchor. Recombinant RGM induces collapse of growth cones of RGCs and guides retinal axons in vitro, demonstrating a repulsive and axon-specific guiding activity [17, 20].

Several studies have been performed to clarify the role of RGMA in the degenerating/non-regenerating processes of CNS injuries: Schwab et al. showed that RGM+ cells accumulated in lesioned and peri-lesional areas after spinal cord injury (SCI), and several glial and non-glial cells and tissues (including the mature and maturing scar) showed RGM immunoreactivity [21]. It was also shown in rats after SCI that inhibition of RGM enhanced growth of injured axons, promoted functional recovery [22], and induced synaptic rearrangements of spared axonal projections [23]. Furthermore, RGMA was found to accumulate at the lesion sites after traumatic brain injury and focal cerebral ischemia [24]. We recently showed that RGMA was present at the crush site after optic nerve crush (ONC) and absent after ONC + lens injury (LI). RGMA was co-localized with nerve fibers, blood vessels, shaft of the ON, astrocytes, oligodendrocytes, and some microglial cells [25]. Moreover, we showed a significantly lowered amount of RGMA in ONC plus LI animals at 2, 4, and 6 days after crush compared to ONC animals [25].

In order to understand the role of RGM in glaucoma, we characterized the expression patterns of the three known members (A, B, C) of the RGM gene family and of the RGMA receptor neogenin in the retina and optic nerve (ON) of a mouse glaucoma model (DBA/2J strain) versus the unaffected C57BL/6J strain [26]. RGMA, RGMB, and neogenin expression were detected in all three nuclear layers of the retina. We found a higher expression of RGMA, RGMB, and neogenin in the retinae of all glaucoma-affected mice than in the age-matched control strain. Furthermore, we detected a higher RGMA and RGMB expression in the ONs of glaucoma-affected DBA/

2J-mice older than 11 months (the age when degeneration of the ON occurs) than in the unaffected control mice of the same age. Although RGMA is expressed in a gradient in the chick retina and blocks only temporal but not nasal axons [17], no gradient has yet been observed in rodents [26–28].

Interestingly, overexpression of neogenin reduced the number of neurons in the developing neural tube, whereas electroporation of *chRGMA* did not cause neuronal death [29]. Simultaneous co-expression of *RGMA* completely suppressed neogenin-induced apoptosis. Moreover, suppression of *chRGMA* expression by siRNA resulted in apoptotic cell death similar to *neogenin* overexpression. Matsunaga et al. concluded a proapoptotic role for neogenin if it is not bound to its ligand RGMA [29]. Moreover, it was recently shown that RGMA promotes retinal ganglion cell survival in vivo and in vitro [30].

In order to better clarify the role of RGMA in the failure of mammal retinal ganglion cells to regenerate their axons after optic nerve injury, we used two models in the present study: a non-regenerating (ONC only) and a regenerating (ONC combined with lens injury (LI)). LI is an established experimental paradigm for reliable long-distance regeneration of mammalian retinal ganglion cell axons [31–33]. We studied the spatio-temporal differences of RGMA and neogenin by performing immunohistochemistry and Western blotting at 6 h, 2, 3, 4, 6, 8, 10, 12, and 20 days post-injury (dpi) in the retina.

## Materials and methods

### Surgical procedures

Surgical procedures were performed as described previously [25]. Briefly, adult male Wistar rats (8–10 weeks old) (Harlan Winkelmann, Germany) were deeply anesthetized by an intraperitoneal injection of a mixture of 100 mg/kg ketamine (CEVA, Germany) and 10 mg/kg xylazine (CEVA, Germany). The ON was surgically exposed in its intraorbital segment. An incision was made in the meninges parallel to the ON in order to separate it from the adjacent central retinal artery to avoid retinal ischemia. ONC was performed using specially designed cross-action tweezers (Fine Science Tools, Germany) for 30 s, always with the same defined pressure. Sham-operated animals were treated the same way except for the actual crush. Lens injury was performed by piercing the lens retrobulbar through the sclera with a 25-gauge needle until the needle was visible through the front of the eye. After the surgical procedures, the skin was sutured and covered with antibiotic ointment. Each animal received only one kind of treatment (ONC + LI, ONC, sham-operated (SHM) plus LI or SHM). Control eyes were taken from untreated animals. All

surgical procedures were performed using a Zeiss OPMI CS microscope (Zeiss, Jena, Germany). Animals were treated according to the Principles of Laboratory Animal Care (NIH publication No. 85–23, revised 1985), the OPRR Public Health Service Policy on the Human Care and Use of Laboratory Animals (revised 1986) and the German animal protection law (Research permission AK7/07 to P.H. and S.S.)

### Immunohistochemistry

For nine time points (6 h, 2, 3, 4, 6, 8, 10, 12, and 20 days post-injury), two treatments were conducted: ONC plus LI and ONC without LI. Additional untreated animals served as controls. Animals SHM + LI, SHM without LI, and LI alone were killed at day 8 post-injury. Eyes were immediately prepared and frozen in Tissue-Tek O.C.T. (Sakura Finetek, Germany) in liquid nitrogen. Frozen sections were longitudinally cut (10–12  $\mu\text{m}$ ) on a cryostat (Leica CM 1900, Germany), thaw-mounted onto glass slides (Superfrost plus, R. Langenbrinck Labor- und Medizintechnik, Germany) and stored at  $-30^\circ\text{C}$  until further use. Immunostaining was performed using standard procedures and described previously [25]. In double-labeling experiments, sections were labeled with antibodies against RGMA or neogenin together with one of the following antibodies: CD68, CD11b, CD45RC, GFAP, neurofilament, CD31, and anti-laminin. Details are listed in Table 1.

Secondary antibodies included anti-mouse IgG, anti-rabbit IgG, and anti-goat IgG antibodies conjugated to Alexa Fluor 488 and Cy3. Details are listed in Table 2. To stain nuclei, some sections were further incubated in a solution containing 0.2  $\mu\text{g}/\text{ml}$  4',6-diamidino-2-phenylindol (DAPI) for 1 min. Stained sections were embedded in FluorSave (Calbiochem, Germany) and imaged using a fluorescent microscope (Axioplan2 imaging<sup>®</sup>, Zeiss, Germany, with the Openlab software, Improvision, Germany). In total, 56 eyes were used for immunostaining. Between two and four eyes

per time point after ONC +/- LI were examined. All double (triple) stainings were always performed with control sections lacking the first antibodies (negative control) that showed no signal. Representative pictures of negative controls are shown in Fig. 11 and 5g.

### Western blotting

To obtain samples for the eight intended time points (6 h, 2, 4, 6, 8, 10, 12, and 20 days post-injury), four treatments were conducted: ONC plus LI, ONC without LI, SHM plus LI, and SHM without LI. Additional untreated animals served as controls. For the ONC animals, four retinæ per time-point were taken, and for the SHM-operated animals, two retinæ per time-point. Always two retinæ were pooled. Western blots and quantification protocols were performed as previously described [25, 34]. Tissues were homogenized with a Dounce homogenizer (Carl Roth, Germany) in RIPA buffer (50 mM Tris-HCl, pH 8; 150 mM NaCl; 1% NP-40; 0.1% SDS; 1:100 Protease inhibitor cocktail Set III, Calbiochem, Germany) and spun at 3,200 rpm for 2 min at  $4^\circ\text{C}$ . The supernatant was removed and frozen in liquid nitrogen and stored at  $-30^\circ\text{C}$  for further use. All work was performed on ice. Concentrations of total protein were determined using a Bradford assay (Bio-Rad Protein Assay, Bio-Rad, Germany) following the manufacturer's protocol.

Equal amounts of protein (10  $\mu\text{g}$ ) were loaded onto 12% SDS gels, followed by transfer to nitrocellulose membranes (Whatman<sup>®</sup> Protran<sup>®</sup>, Whatman, Germany). Membranes were incubated in 2% BSA for 1 h at room temperature, followed by incubation with primary antibody overnight at  $4^\circ\text{C}$  (actin-antibody 1 h). The same blots were stained unstripped in this order: anti-RGMA, anti-neogenin, and anti-actin. Concentrations of the primary antibodies were: anti-RGMA: 1:1000, anti-neogenin 1:1000 (both: R&D Systems, Germany), anti-actin: 1:10 000 (Chemicon, Temecula, CA, USA). Secondary

**Table 1** Antigen, source, and dilution of the primary antibodies used for immunostaining

Antigen or kind of cell	Antibody (ab)	Source	Catalog no.	Dilution
RGMA	RGMA polyclonal ab	R&D Systems, Germany	AF2458	1:60
Neogenin	Neogenin polyclonal ab		AF1079	1:200
RGC/axons/nerve fibers	Neurofilament 200 phosphorylated and non-phosphorylated monoclonal ab (mNF)	Sigma, Germany	N0142	1:300
Microglia, macrophages, dendritic cells, granulocytes	CD11b (OX42) monoclonal ab	AbD Serotec, Germany	MCA275R	1:500
Lymphocytes	CD45RC (OX22) monoclonal ab		MCA53R	1:500
Astrocytes/activated Müller cells	Glial fibrillary acidic protein (GFAP) polyclonal ab	Dako-Cytomation, Germany	Z0334	1:7000
Basal laminae and the glia limitans externa	Anti-laminin polyclonal ab	BD Pharmingen, Germany	Z0097	1:100
Endothelial cells, platelets and subsets of leukocytes	CD31 (PECAM-1) monoclonal ab		555025	1:100

**Table 2** Antigen, source, and dilution of the secondary antibodies used for immunostaining

With primary ab	Antibody (ab)	Source	Catalog no.	Dilution
RGMA, Neogenin	Cy3 conjugated donkey anti-goat IgG	Dianova, Germany	705-165-147	1:2000
CD11b, CD45RC, mNF, CD31	Alexa488 conjugated Donkey anti-mouse IgG	Invitrogen, Germany	A21202	1:1000
GFAP, laminin	Alexa488 conjugated donkey anti-rabbit IgG		A21206	1:2000

antibodies were applied for 1 h at room temperature: peroxidase-conjugated rabbit anti-goat IgG 1:40 000 for RGMA and 1:50000 for neogenin (Calbiochem, Germany) and peroxidase-conjugated goat anti-mouse IgG; 1:100000 (Calbiochem, Germany). All antibodies were diluted in blocking solution. Chemiluminescence was detected using the ECL chemiluminescence system (Pierce/Thermo Fisher Scientific, Germany), followed by exposure of the membranes to X-ray films (GE Healthcare, Germany). Protein ratios were calculated based on densitometrical quantification of scanned films using ImageJ (<http://rsb.info.nih.gov/ij/>), with a minimum of three measurements per protein. RGMA and neogenin protein levels were normalized to actin levels and to levels of a control animal sample, considering error propagation of the standard deviations, also in further normalizations to SHM animals. Significances of the differences between the values were calculated using a *t* test. To exclude technical artefacts, we performed the experiments for the ONC and ONC + LI treatments with a second set of animals. Isotypic IgG controls were performed showing no binding to any band detected with the RGMA or neogenin antibody (Supplemental data 1a and 2a). Non-specific binding of the second antibody was excluded (supplemental data 1b and 2b).

## Results

### RGMA in the rat retina

#### *RGMA and retinal ganglion cells and nerve fibers*

Independent of the treatment, RGMA was localized in the nuclear layers (NLs), the plexiform layers (PLs), the nerve fiber layer (NFL), and in retinal ganglion cells (RGC) (Fig. 1a–k). In the LI animals, RGMA staining was fainter in the inner plexiform layer compared to the crushed or SHM only animals (Fig. 1a vs. b and f vs. g). A high amount of RGMA was found on the outer side of the ONL (Fig. 1c) and on the inner side of the INL (Fig. 1d) in all retinæ. Nerve fibers are always RGMA+ (Fig. 1a–k). However, the amount of RGCs decreases with ongoing time after the crush, and also lesser nerve fibers are present (Fig. 1a, i, k). However, in ONC + LI animals, many

RGMA+ RGCs survive the optic nerve crush (Fig. 1i vs. j). Twenty days post-crush only RGMA+ cells, which are not RGCs, are present in the area where formerly RGC were situated (Fig. 1k).

#### *RGMA and microglia*

Retinæ from crushed optic nerves displayed a high amount of enlarged CD11b+ microglia (Fig. 2a), whereas almost no activated microglial cells were found in control or SHM animals (Fig. 2b). In the retinæ of ONC + LI animals, fewer CD11b+ microglial cells were found than in ONC only animals, but more than in SHM or control animals (data not shown). Many but not all microglial cells are RGMA+ (Fig. 2c). RGMA+ cells that are present in the GCL 20 days after ONC are often RGMA+ microglia (Fig. 2c).

#### *RGMA and astrocytes/Müller cells*

After ONC (Fig. 3a, b) or ONC + LI (data not shown), a higher GFAP expression can be seen by Müller cells and astrocytes compared to SHM (Fig. 3c) or control animals (data not shown), where only astrocytes are GFAP+. All investigated astrocytes were RGMA+ (Fig. 3a–c). Indeed, the DAPI staining allows us to differentiate between the end-feet of the Müller cells and the cell bodies of the astrocytes located in the GCL (Fig. 3b). Based on these results, it can be concluded that, besides the aforementioned microglia, astrocytes also belong to the population of the RGMA+ cells found in the former ganglion cell layer of late crushed rat retinæ, e.g., 12 or 20 days after crush (Fig. 1i, k).

#### *RGMA and blood vessels or lymphocytes*

Retinal blood vessels were RGMA+ (data not shown). No lymphocytes invading the retina were found (data not shown).

#### *Quantification of RGMA in the retina*

Three secreted or truncated isoforms of RGMA were present in Western blots: A ~43-kDa, a ~35-kDa, and a

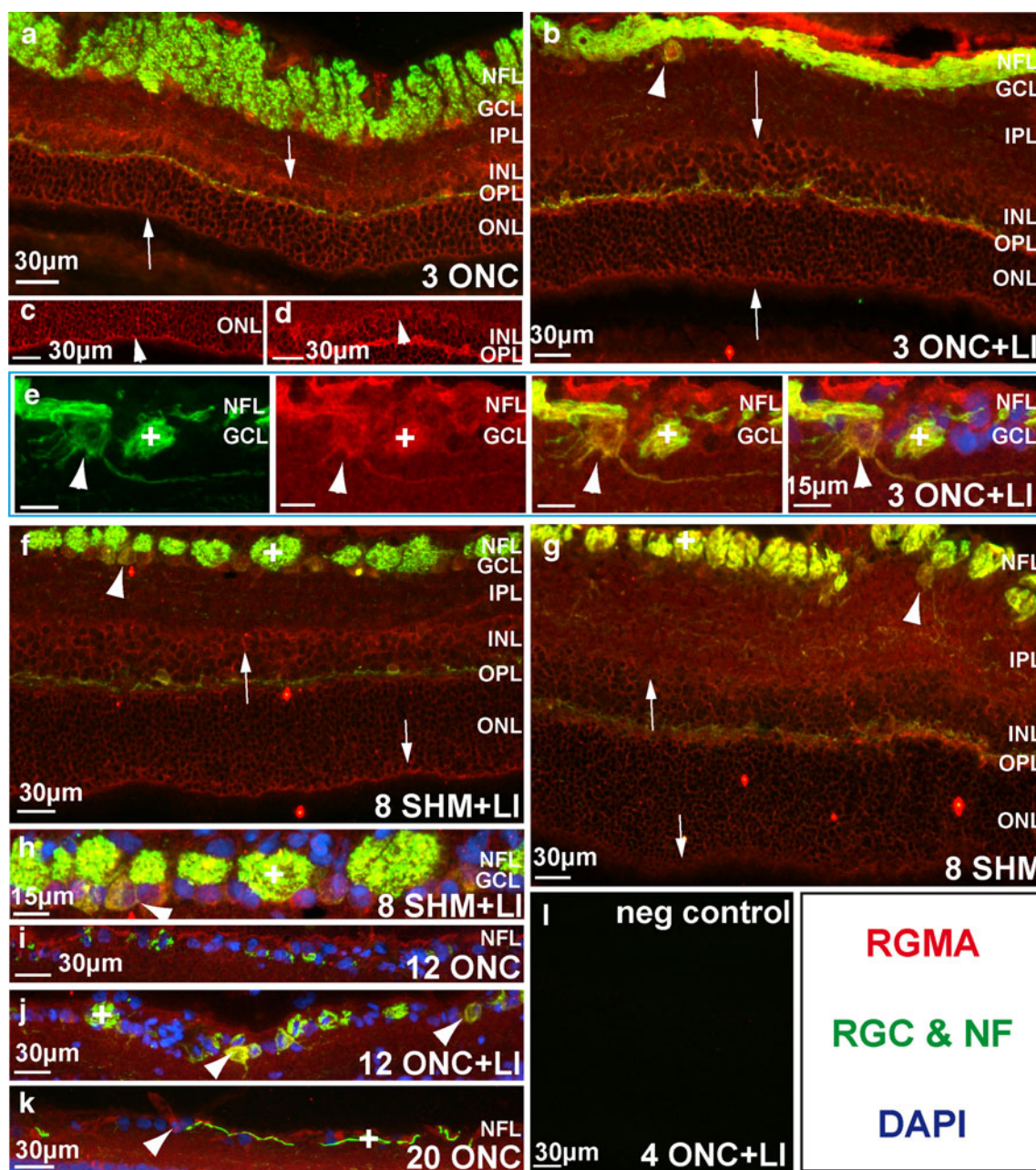


**Fig. 1** Representative images of RGMA (red) and neurofilament (green) staining in the retina. **a–k** RGMA was found in the nerve fiber layer (NFL), the ganglion cell layer (GCL), the inner and outer plexiform layers (IPL and OPL), and in the inner and outer nuclear layers (INL and ONL) in all investigated retinæ independent of the treatment. **a** Retina shows the typical RGMA pattern 3 days after crush: Both plexiform layers show a very high amount of RGMA. In the PLs, RGMA is ubiquitous, whereas RGMA is restricted to the membranes of the cells in the NLs. **a–d, f, g** At all investigated stages, RGMA is more highly expressed on the inner side of the INL and the outer side of the ONL (arrows). **b** The same can be seen in a retina 3 days after ONC + LI, except for the IPL where RGMA immunoreactivity is a little bit weaker. **e** Retinal ganglion cells (arrowhead) and nerve fibers (+) are always RGMA+. The amount of RGMA is higher in the nerve fibers than in the RGC. They can easily be identified by their morphology, the amount of RGMA and DAPI staining (in blue, most right picture). **f** In the SHM + LI animals,

RGMA+ RGCs (arrowhead) and nerve fibers (+) are visible. **g** The sham-operated animals show no differences in the general RGMA pattern compared to the operated animals except for the NFL, GCL, and the amount of RGCs (arrowhead). **h–k** Compared to the SHM + LI operated animals, the loss of RGC and nerve fibers is obvious in the retina 12 days post-crush, and since RGC are RGMA+, also a decrease in the number of RGMA+ cells is visible, whereas in the ONC + LI animal more RGCs (arrowheads) and nerve fibers (+) are present. Twenty days post crush, no RGCs are visible, and only a few left over nerve fibers (+). Nevertheless, there are still RGMA+ cells beneath the NFL. Most of them are astrocytes and microglia as shown in the other figures (Figs. 2c and 3b). **l** The negative control of the double staining showed no RGMA or neurofilament signal. In this and in the following immunohistochemical images, the treatment and time-points are indicated in the lower right corner of every image. Please note that for a clearer image representation the DAPI staining was only included when it was useful for better understanding

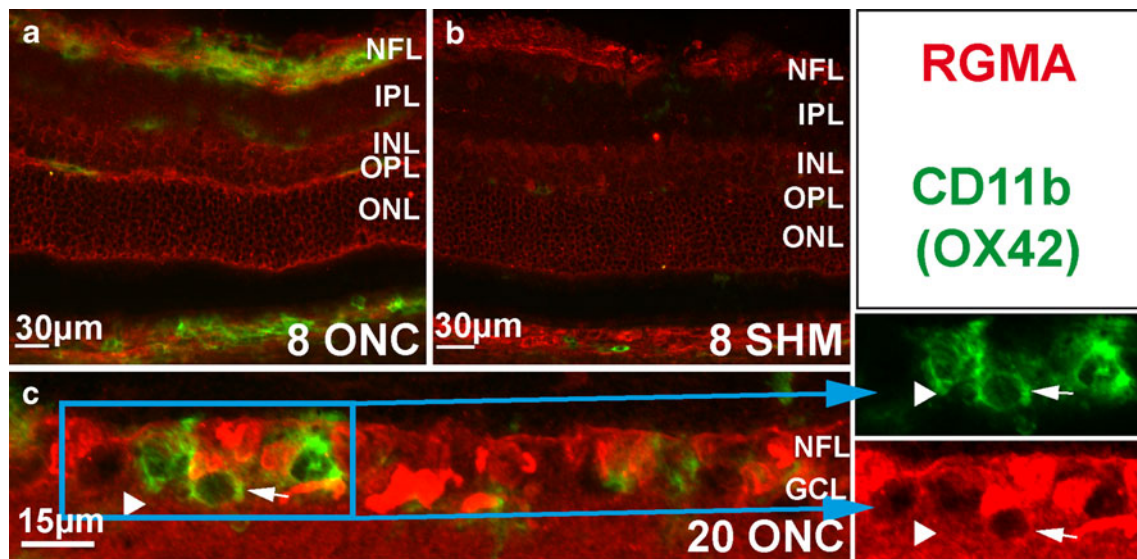


**Fig. 2** Representative images of RGMA (red) and CD11b (green) staining in the retina (a). Eight days post-ONC, animals have a lot of activated microglia in their retina, especially near the RGCs, whereas they are absent in the SHM animals (b). c Images of CD11b and RGMA staining and the overlay show a clear co-localization of

CD11b and RGMA at the membrane of a microglial cell (arrow). Other RGMA+ but not CD11b+ cells are also visible (arrowhead). The treatment and time-points are stated in the lower right corner of every image

~27-kDa band (Fig. 4a). Several more bands were found in the lower molecular mass range beyond the ~27-kDa band in animals with LI independent of the crush (Fig. 4a). We assume that these additional bands could be the result of further cleavage of RGMA caused directly or indirectly by LI. We quantified the blots to see differences with different settings: one set of measurements was performed with the three RGMA bands described and the other set with the three bands including the cleavage products. Normalization to actin (Fig. 4b) and the untreated control (Fig. 4a) placed on every blot showed no significant differences in seven out of eight time-points measured with the cleavage products (indicated by the first black box in Fig. 4a) and six out of eight time-points measured without the cleavage

products (indicated by the second black box in Fig. 4a) between the SHM, SHM + LI, and ONC animals (data not shown). The amount of RGMA in ONC + LI animals, however, was significantly higher from 6 h to 6 days and 20 days post-crush (including cleavage products) but only significant higher at time points 6 h, 4, 10, and 20 days post crush, when measurements were performed without the cleavage products (data not shown). Further normalization to the corresponding SHM confirmed the results: The first set of measurements (including potential cleavage products) showed that the amount of RGMA is almost always higher in the ONC + LI animals (except for the 12 days after ONC animals) (Fig. 4c). The second set of measurements performed without the cleavage products revealed that the

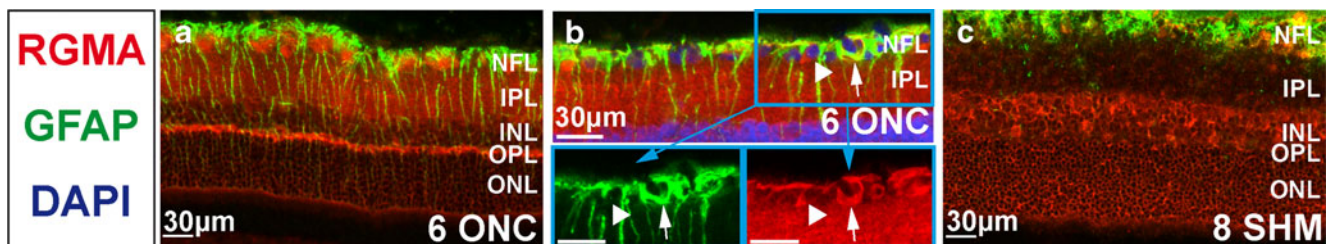


**Fig. 3** Representative images of RGMA (red) and GFAP (green) staining in the rat retina. a After ONC or ONC + LI, a GFAP-up-regulation can be observed in the retina, in particular by the Müller cells. (b and inserts) RGMA+, GFAP+ and DAPI+ (blue) stained cells in the GCL/NFL are astrocytes (arrow). Other RGMA+ and DAPI+ but not GFAP+ cells are visible close to the astrocytes (arrowhead). These are probably RGCs or microglial cells. Not DAPI-stained, but RGMA+ and

GFAP+ tissue are the end-feet of Müller cells or the processes of astrocytes. c In the SHM animals, GFAP is not up-regulated in the Müller cells and astrocytes are weaker RGMA+ and GFAP+. The treatment and time-points are stated in the lower right corner of every image. Please note that for a clearer image representation, the DAPI staining was only included when it was useful for better understanding

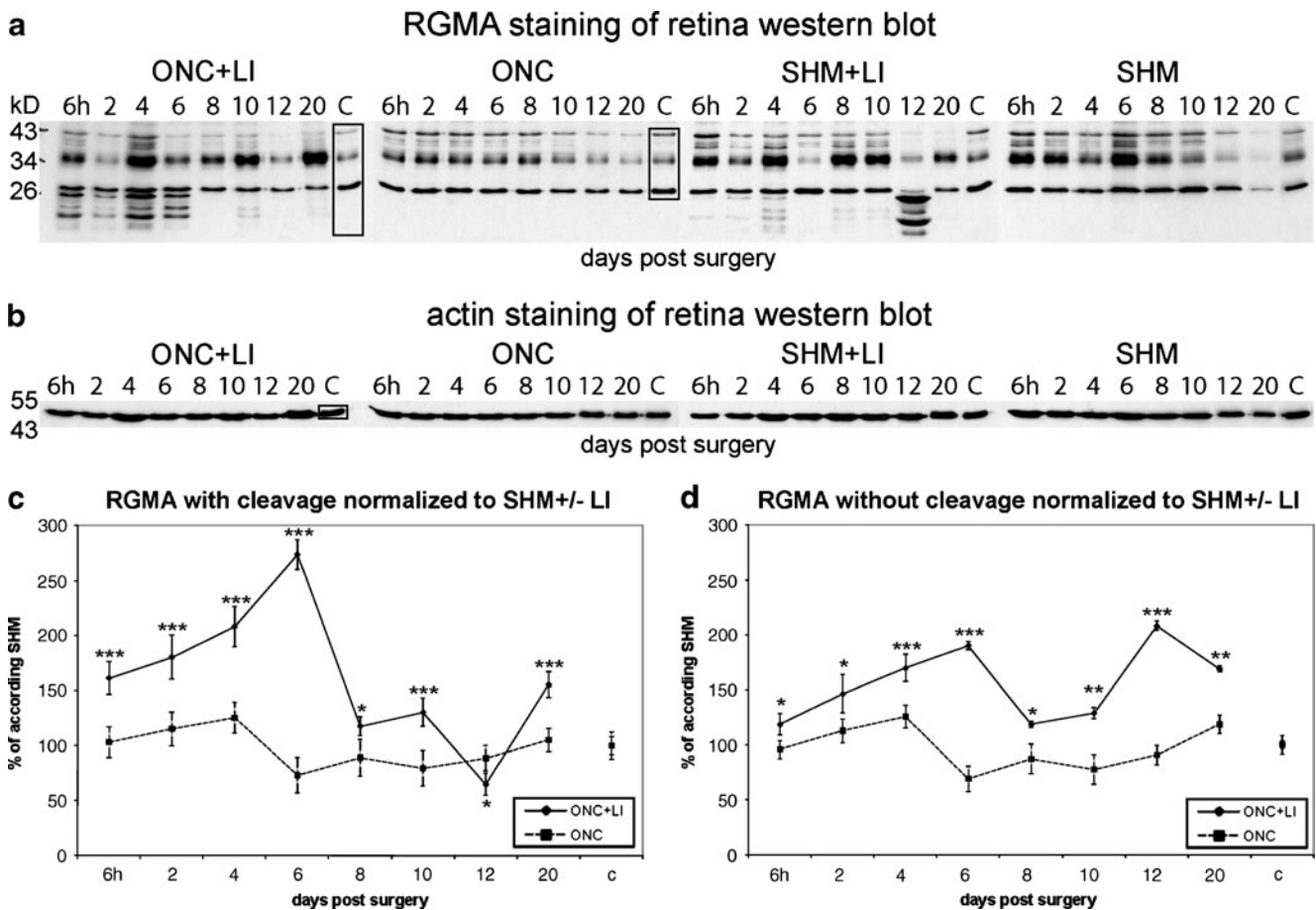


**Fig. 4** Western blots and quantification of RGMA in the retina. **a** Western Blots show several RGMA isoforms, a ~43-kDa, a ~35-kDa, and a ~27-kDa isoform. The proprotein was not found at any stage observed. Several additional bands are visible beneath the 27-kDa band, only in LI animals independent of crush. These bands are probably the result of degradation of RGMA caused by LI. The first *black frame* indicates the area that was quantified including the cleavage products and the second frame the area that was quantified without the cleavage products. **b** The similar actin bands demonstrate an equal loading of the gel. The *black frame* indicates the area that was quantified for normalization. **c** The three RGMA bands and the potential cleavage products were quantified and normalized to the

corresponding actin band and the control animals band “C” located on each blot and further to the corresponding SHM (ONC + LI to SHM + LI and ONC to SHM). An increase of RGMA in the ONC + LI retina from 6 h post-crush to 6 days post-crush can be seen, whereas a decrease is obvious afterwards. The amount of RGMA in ONC + LI animals remained higher than in ONC animals (except for 12 days post-crush). **d** The same normalization without the cleavage products showed an amount of RGMA that was always higher in the ONC + LI animals compared to the ONC only animals. The *error bar* represents standard deviation. *p* values are indicated as follows: \*  $p < 0.05$ , \*\*  $p < 0.01$ , \*\*\*  $p < 0.001$

amount of RGMA is always higher in the ONC + LI animals compared to the ONC animals (Fig. 4d).

#### Neogenin in the rat retina

##### *Neogenin and retinal ganglion cells and nerve fibers*

The neogenin protein pattern was congruent to the RGMA pattern independent of the treatment (Fig. 5). Even the higher presence at the inner INL and outer ONL was congruent (Fig. 5a, b, f). In Fig. 5c–e, cross-sectioned nerve fiber bundles (marked by a +) are visible with strong NF and a clear neogenin immunoreactivity, whereas the RGCs show no staining of the soma (*arrowhead*).

#### *Quantification of neogenin in the retina*

Two isoforms of approximately 180 and 190-kDa were found (Fig. 6a). The measurements of the neogenin blots were also normalized to actin (Fig. 6b) and a control animal placed on every blot (Fig. 6a, b). The amount of neogenin varied between 50 and 150% of the control animals for all treatments, except for five time points: neogenin was considerably lowered at 6 h after ONC, whereas it was higher than average at the time points 6 h ONC + LI, 2 days ONC, 4 days ONC + LI, and 20 days ONC + LI (data not shown). Normalization to the corresponding SHM showed a significant higher amount of neogenin in the ONC animals at time points 6 h (ONC 40%, ONC + LI 140%;

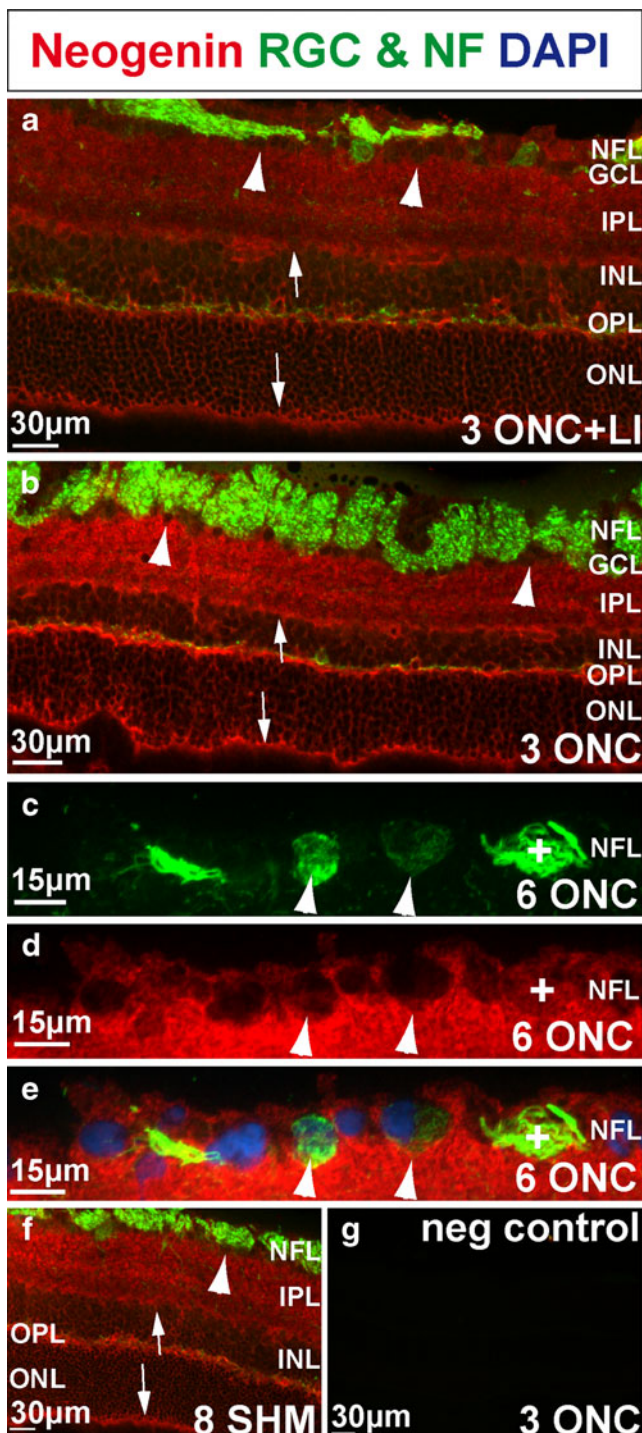


**Fig. 5** Representative images of neogenin (*red*) and neurofilament (*green*) in the rat retina. **a–f** Neogenin was found in the nerve fiber layer (NFL), the ganglion cell layer (GCL), the inner and outer plexiform layers (IPL and OPL), and in the inner and outer nuclear layers (INL and ONL) in all investigated retinæ independent of the treatment. The neogenin pattern is congruent with the RGMA pattern at all stages investigated, including the higher amount at the edges of the nuclear layers (*arrows*). **c–f** The RGCs (*arrowheads*), however, are never neogenin+. Nerve fiber bundles (+) show a clear neogenin immunoreactivity. **g** The negative control of the double staining showed no signal. The treatment and time-points are stated in the lower right corner of every image. Please note that for a clearer image representation, the DAPI staining was only included when it was useful for better understanding

## Discussion

We studied differences in the protein patterns of RGMA in the regenerating (ONC + LI) vs. the non-regenerating (ONC) model. In the retina, astrocytes, microglial cells, blood vessels, nerve fibers, RGC and cells of the NLs with their processes in the PLs were found to be RGMA+. Outer and inner segments of photoreceptors were never RGMA+. Upregulation of GFAP including an activation of the Müller cells in the retina after LI or optic nerve trauma has been reported by many groups [33, 35–40]. Furthermore, it has been reported that LI-induced upregulation of astrocyte-derived CNTF switches RGC into a regenerative state [41]. Microglia is naturally present in both the retina and the optic nerve and may become activated under several circumstances [42–45].

A persistent presence of RGMA in the CNS of mature animals unaffected by injuries or chronic diseases has been reported by several authors [28, 46]. Schwab et al. investigated the RGMA protein pattern after SCI in rats and after traumatic brain injury/focal cerebral ischemia in humans [21, 24]. In untreated control animals, RGMA was co-localized to myelin fibers and oligodendrocytes [21]. In the healthy adult human brain, RGMA was located on the perikarya of some neurons, choroid plexus, smooth muscle of the vasculature, endothelial cells, and on oligodendrocytes and white matter fiber tracts [24]. In SCI animals, RGMA+ cells and structures were microglia/macrophages, components of the developing scar, astrocytes, neurons, fibroblasts, axonal-like bulbs, neo-laminae, smooth muscle/endothelial cells, etc., but not lymphocytes [21]. RGMA accumulated in the infarct core, peri-infarctional areas of the penumbra, and hemorrhagic areas of focal cerebral ischemia patients or lesion site, mature scar, or glial scar of traumatic brain injury patients. Lesion-associated cellular RGMA staining was confined to neurons, a few reactive astrocytes, invading leukocytes (granulocytes, monocytes, lymphocytes), and blood vessels [24].

$p < 0.001$ ), 2 days (ONC 310%, ONC + LI 55%;  $p < 0.001$ ), 8 days (ONC 155%, ONC + LI 90%;  $p < 0.001$ ), 20 days (ONC 200%, ONC + LI 290%;  $p < 0.001$ ). At days 4 ( $p < 0.05$ ), 6 ( $p < 0.01$ ) and 10 ( $p < 0.01$ ), the amount of neogenin in ONC + LI animals was significantly higher than in ONC (Fig. 6c).



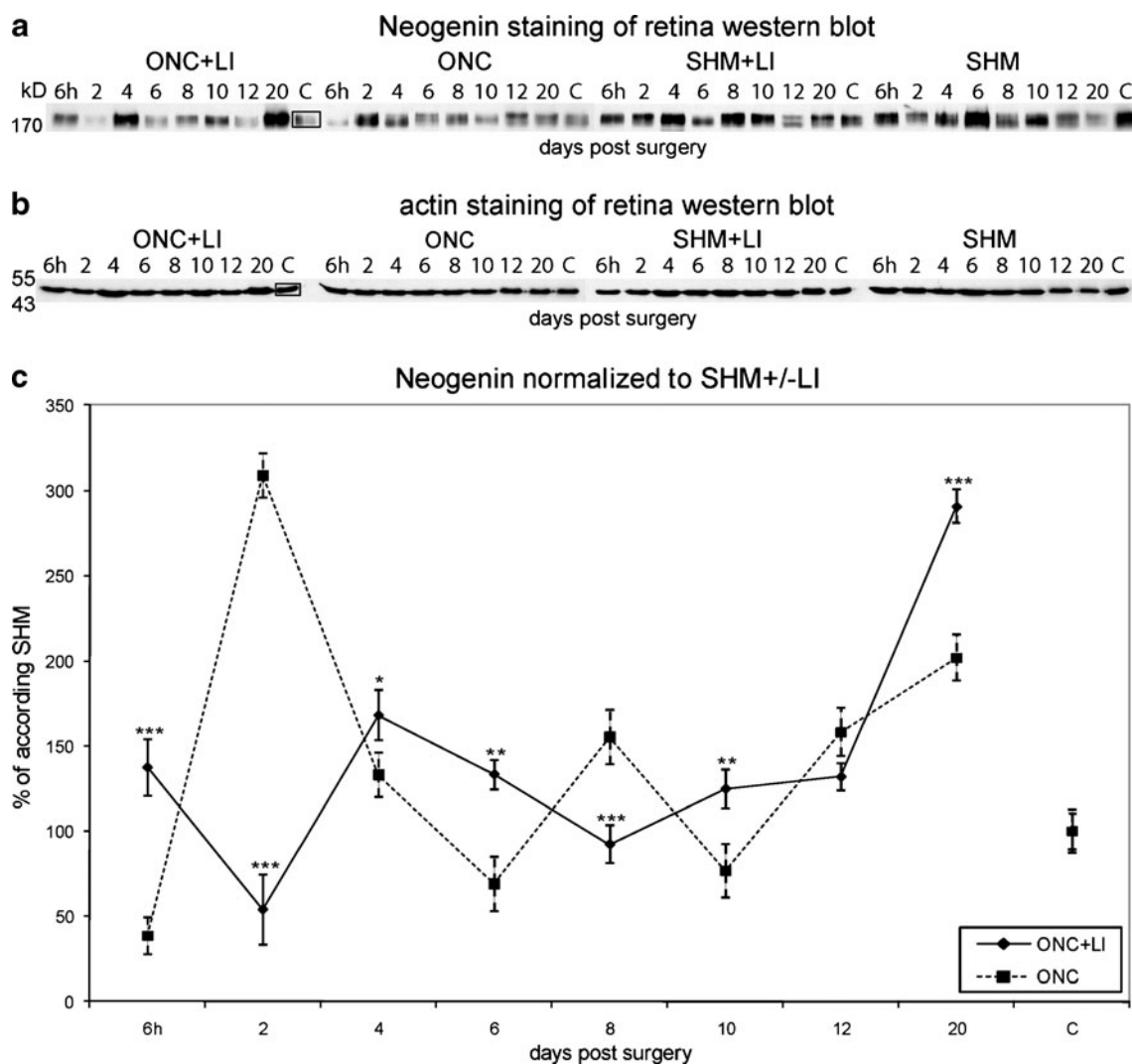


**Fig. 6** Western blots and quantification of neogenin in the retina. **a** Western blots showed two isoforms, a 180-kDa and a 190-kDa isoform (Fig. 6a). The black frame indicates the area that was quantified. **b** Actin bands demonstrate an equal loading. The black frame indicates the area that was quantified for normalization. **c** The two neogenin bands were quantified and normalized to their

corresponding actin band and the control animals band “C” located on each blot and further to the corresponding SHM (ONC + LI to SHM + LI and ONC to SHM). Significant differences were observed in seven out of eight time points. Error bar represents standard deviation. *p* values are indicated as follows: \*  $p < 0.05$ , \*\*  $p < 0.01$ , \*\*\*  $p < 0.001$

Inhibition of RGMA in rats after SCI enhanced growth of injured axons, promoted functional recovery [22], and induced synaptic rearrangements of spared axonal projections [23]. Thus, re-expression of embryonic repulsive cues in adult tissues contributes to a failure of axon regeneration in the central nervous system [47].

We localized RGMA at the crush site immediately after ONC alone, and RGMA remained present from there on, whereas it was always absent in the ONC + LI animals [25]. In all investigated groups (including control and sham animals), many cells were found to be RGMA<sup>+</sup> in the ON: nerve fibers, blood vessel endothelial cells, astrocytes,

oligodendrocytes, some microglial cells, and the shaft of the optic nerve. Neogenin was never found at the crush site. Nerve fibers were faintly to strongly neogenin<sup>+</sup>.

The RGMA and neogenin protein patterns found in the rat retina are comparable to the results reported in a previous publication of our group, in which we analyzed the RNA expression patterns of RGMA and neogenin in DBA/2J and C57BL/6J mice by in-situ hybridization [26]. We found RNA expression of RGMA and neogenin in the ganglion cell layer (GCL), in the inner nuclear layer (INL), the outer nuclear layer (ONL), and in the ON. In addition to these layers, both proteins were also found in the plexiform

layers in our rat model because the proteins are distributed into the cell processes in contrast to the RNA, which was restricted to the soma. Here, also no RGMA or neogenin protein was found in the inner and outer segments of the photoreceptors. The higher expression/amount of RGMA observed in the inner INL and outer ONL (see arrows in Fig. 1, in particular c, d) was also present in both investigated mouse strains [26].

The neogenin pattern in our ONC, ONC + LI, SHM or SHM + LI-operated animals was unchanged compared to the pattern of untreated animals in a recent publication [30]. Koeberle et al. reported a clear staining of RGC somata and a weak staining of nerve fibers. Unfortunately, we can neither in our picture nor in their publication see a positive staining of RGCs in retina sections, especially as they did not perform double staining to identify RGCs or nerve fibers. We clearly saw a definite co-staining of neogenin and nerve fibers in the retina (Fig. 5) and in the optic nerve [25]. However, we cannot exclude that the membranes of the RGCs were neogenin+ as it is not possible to distinguish this staining from the general staining in the GCL or IPL. The somata were not clearly neogenin+. In contrast, Koeberle et al. showed a double staining of RGCs/neogenin and nerve fibers/neogenin in their in-vitro data. This discrepancy cannot be explained. Regarding the Western blots, several interesting effects have been observed: RGMA degradation, cleavage, truncation, or secretion in the retina occur after LI independent of a crush. Since the antibody used in our study is polyclonal and no band was missing in the Western blot of ONC + LI animal's samples, it is not clear which form of RGMA is cleaved into fragments. We did not observe these cleaved forms of RGMA found in the retina's Western blots of this study in the ON's Western blots in our previous study [25].

Western blots lacking the first antibody and blots with an isotopic control never showed these cleavage products (Supplemental data 1a, b). Furthermore, we completely redid the experiments for the ONC and ONC + LI treatments with different animals, and the same effects occurred (data not shown). Moreover, database searches with the sequences of the protein the RGMA antibody were generated against, did not reveal any potential binding to any other proteins present in the eye. Therefore, we exclude technical artefacts as a reason for the occurrence of cleavage products.

Studies in the direction of targeting either the N-terminal or the C-terminal part or the (pro-)protein are necessary to evaluate any possible effect of RGMA degradation.

Cleaved, truncated, and soluble isoforms, as well as the proprotein of RGMs, have been reported in several studies under different conditions and with different species and models [27, 48–52], whereas Western blots of cell culture and/or after PI-PLC digest showed only the cleaved isoform, e.g., [17, 22, 53].

The data in this study and our recently published study [25] suggest opposing effects of RGMA in the retina and the optic nerve. The growth-inhibiting effects have been discussed before. Since 2004, several publications have described anti-apoptotic effects of RGMA, or, to be more precise, a pro-apoptotic effect of the receptor neogenin [29, 30, 54, 55]. In summary, this and our previous study corroborate these findings. Several results from the literature and our data seem to be contradictory, however, this is not the case: on the one hand, RGMA has an influence on the growth cones, and on the other side on cell somata [20–22, 25, 29, 30, 51, 54–57].

Interestingly, opposing effects in the optic nerve (growth inhibition) vs. the retina (growth promotion) were also shown for the repulsive molecule Nogo [58, 59].

The two neogenin isoforms are in accordance with the literature mentioning a 190-kDa isoform and a “shorter form” [60]. The huge differences between the neogenin levels in the first 48 h between ONC +/- LI in the Western blots may be a sign for the different processes affecting neogenin after crush and LI: The expression of neogenin in growth cones has been reported for several in vitro and in vivo systems [56, 61]. Therefore, a change in the neogenin expression could occur due to the initiation of growth cone regrowth, which normally secretes a small amount of neogenin. This effect may be altered by the death of their RGC somata. Moreover, it might be speculated that the high neogenin value measured 48 h after crush in ONC animals might be associated with the previously mentioned induction of apoptosis via neogenin.

Furthermore, neogenin was reported to be regulated by Pax6 [62]. Although it has not been reported that Pax6 is influenced by LI, it can be assumed that Pax6 as a key factor in lens development [62, 63] may also be influenced by LI. The influence on Pax6 would then change the neogenin expression, which could also have an impact on RGMA.

Our results indicate that the RGMA protein pattern is altered in the regenerating vs. the non-regenerating model, although the changes in the spatial pattern seem to be restricted to the RGC layer. The results of the Western blots show a clear upregulation of RGMA in the regenerating model vs. the non-regenerating model and therefore contribute to the several publications that RGMA has a potential neuroprotective/anti-apoptotic function. Further experiments should be performed to define the fragments, into which RGMA is cleaved, and the mechanisms of cleavage.

**Acknowledgements** The authors thank Marcel Alavi (Molecular Genetics Laboratory, Institute for Ophthalmic Research, Centre for Ophthalmology, Röntgenweg 11, 72076 Tübingen, Germany) for his excellent advice concerning the Western blots. The authors also thank Sigrid Henke-Fahle (Centre for Ophthalmology, University Eye

Hospital, Schleichstr. 12/1, 72076 Tübingen, Germany) for her excellent advice in experimental strategies and design. The authors thank the Else Kröner-Fresenius-Stiftung (P40/08//A32/08) for supporting Sven Schnichels. All authors disclose that there are no commercial interests in the subject of the manuscript or in entities discussed in the manuscript.

## References

- Mey J, Thanos S (1993) Intravitreal injections of neurotrophic factors support the survival of axotomized retinal ganglion cells in adult rats in vivo. *Brain Res* 602:304–317
- Berkelaar M, Clarke DB, Wang YC, Bray GM, Aguayo AJ (1994) Axotomy results in delayed death and apoptosis of retinal ganglion cells in adult rats. *J Neurosci* 14:4368–4374
- Fischer D, Pavlidis M, Thanos S (2000) Cataractogenic lens injury prevents traumatic ganglion cell death and promotes axonal regeneration both in vivo and in culture. *Invest Ophthalmol Vis Sci* 41:3943–3954
- Heiduschka P, Fischer D, Thanos S (2004) Neuroprotection and regeneration after traumatic lesion of the optic nerve. *Klin Monatsbl Augenheilkd* 221:684–701
- Villegas-Perez MP, Vidal-Sanz M, Rasminsky M, Bray GM, Aguayo AJ (1993) Rapid and protracted phases of retinal ganglion cell loss follow axotomy in the optic nerve of adult rats. *J Neurobiol* 24:23–36
- Parrilla-Reverter G, Agudo M, Sobrado-Calvo P, Salinas-Navarro M, Villegas-Perez MP, Vidal-Sanz M (2009) Effects of different neurotrophic factors on the survival of retinal ganglion cells after a complete intraorbital nerve crush injury: a quantitative in vivo study. *Exp Eye Res* 89:32–41
- Peinado-Ramon P, Salvador M, Villegas-Perez MP, Vidal-Sanz M (1996) Effects of axotomy and intraocular administration of NT-4, NT-3, and brain-derived neurotrophic factor on the survival of adult rat retinal ganglion cells. A quantitative in vivo study. *Invest Ophthalmol Vis Sci* 37:489–500
- Nadal-Nicolas FM, Jimenez-Lopez M, Sobrado-Calvo P, Nieto-Lopez L, Canovas-Martinez I, Salinas-Navarro M, Vidal-Sanz M, Agudo M (2009) Brn3a as a marker of retinal ganglion cells: qualitative and quantitative time course studies in naive and optic nerve-injured retinas. *Invest Ophthalmol Vis Sci* 50:3860–3868
- Selles-Navarro I, Ellezam B, Fajardo R, Latour M, McKerracher L (2001) Retinal ganglion cell and nonneuronal cell responses to a microcrush lesion of adult rat optic nerve. *Exp Neurol* 167:282–289
- Caroni P (1997) Intrinsic neuronal determinants that promote axonal sprouting and elongation. *Bioessays* 19:767–775
- Fournier AE, GrandPre T, Strittmatter SM (2001) Identification of a receptor mediating Nogo-66 inhibition of axonal regeneration. *Nature* 409:341–346
- Wizenmann A, Thies E, Klostermann S, Bonhoeffer F, Bahr M (1993) Appearance of target-specific guidance information for regenerating axons after CNS lesions. *Neuron* 11:975–983
- Cramer SC, Chopp M (2000) Recovery recapitulates ontogeny. *Trends Neurosci* 23:265–271
- Knoll B, Drescher U (2002) Ephrin-As as receptors in topographic projections. *Trends Neurosci* 25:145–149
- Pasterkamp RJ, Verhaagen J (2006) Semaphorins in axon regeneration: developmental guidance molecules gone wrong? *Philos Trans R Soc Lond B Biol Sci* 361:1499–1511
- Low K, Culbertson M, Bradke F, Tessier-Lavigne M, Tuszynski MH (2008) Netrin-1 is a novel myelin-associated inhibitor to axon growth. *J Neurosci* 28:1099–1108
- Monnier PP, Sierra A, Macchi P, Deitinghoff L, Andersen JS, Mann M, Flad M, Hornberger MR, Stahl B, Bonhoeffer F, Mueller BK (2002) RGM is a repulsive guidance molecule for retinal axons. *Nature* 419:392–395
- Muller BK, Jay DG, Bonhoeffer F (1996) Chromophore-assisted laser inactivation of a repulsive axonal guidance molecule. *Curr Biol* 6:1497–1502
- Stahl B, Muller B, von Boxberg Y, Cox EC, Bonhoeffer F (1990) Biochemical characterization of a putative axonal guidance molecule of the chick visual system. *Neuron* 5:735–743
- Rajagopalan S, Deitinghoff L, Davis D, Conrad S, Skutella T, Chedotal A, Mueller BK, Strittmatter SM (2004) Neogenin mediates the action of repulsive guidance molecule. *Nat Cell Biol* 6:756–762
- Schwab JM, Conrad S, Monnier PP, Julien S, Mueller BK, Schluessener HJ (2005) Spinal cord injury-induced lesional expression of the repulsive guidance molecule (RGM). *Eur J Neurosci* 21:1569–1576
- Hata K, Fujitani M, Yasuda Y, Doya H, Saito T, Yamagishi S, Mueller BK, Yamashita T (2006) RGMA inhibition promotes axonal growth and recovery after spinal cord injury. *J Cell Biol* 173:47–58
- Kyoto A, Hata K, Yamashita T (2007) Synapse formation of the cortico-spinal axons is enhanced by RGMA inhibition after spinal cord injury. *Brain Res* 1186:74–86
- Schwab JM, Monnier PP, Schluessener HJ, Conrad S, Beschoner R, Chen L, Meyermann R, Mueller BK (2005) Central nervous system injury-induced repulsive guidance molecule expression in the adult human brain. *Arch Neurol* 62:1561–1568
- Schnichels S, Heiduschka P, Julien S (2011) Different spatial and temporal protein expressions of repulsive guidance molecule a and neogenin in the rat optic nerve after optic nerve crush with and without lens injury. *J Neurosci Res* 89:490–505
- Schnichels S, Conrad S, Warstat K, Henke-Fahle S, Skutella T, Schraermeyer U, Julien S (2007) Gene expression of the repulsive guidance molecules/neogenin in the developing and mature mouse visual system: C57BL/6 J vs. the glaucoma model DBA/2 J. *Gene Expr Patterns* 8:1–11
- Niederkofler V, Salie R, Sigrist M, Arber S (2004) Repulsive guidance molecule (RGM) gene function is required for neural tube closure but not retinal topography in the mouse visual system. *J Neurosci* 24:808–818
- Schmidtmer J, Engelkamp D (2004) Isolation and expression pattern of three mouse homologues of chick Rgm. *Gene Expr Patterns* 4:105–110
- Matsunaga E, Tauszig-Delamasure S, Monnier PP, Mueller BK, Strittmatter SM, Mehlen P, Chedotal A (2004) RGM and its receptor neogenin regulate neuronal survival. *Nat Cell Biol* 6:749–755
- Koerberle PD, Tura A, Tasew NG, Schlichter LC, Monnier PP (2010) The repulsive guidance molecule, RGMA, promotes retinal ganglion cell survival in vitro and in vivo. *Neuroscience* 169:495–504
- Fischer D, Heiduschka P, Thanos S (2001) Lens-injury-stimulated axonal regeneration throughout the optic pathway of adult rats. *Exp Neurol* 172:257–272
- Lorber B, Berry M, Hendriks W, den Hertog J, Pulido R, Logan A (2004) Stimulated regeneration of the crushed adult rat optic nerve correlates with attenuated expression of the protein tyrosine phosphatases RPTPalph, STEP, and LAR. *Mol Cell Neurosci* 27:404–416
- Leon S, Yin Y, Nguyen J, Irwin N, Benowitz LI (2000) Lens injury stimulates axon regeneration in the mature rat optic nerve. *J Neurosci* 20:4615–4626
- Alavi MV, Bette S, Schimpf S, Schuettauf F, Schraermeyer U, Wehrl HF, Ruttiger L, Beck SC, Tonagel F, Pichler BJ, Knipper M, Peters T, Laufs J, Wissinger B (2007) A splice site mutation in the murine Opa1 gene features pathology of autosomal dominant optic atrophy. *Brain* 130:1029–1042

35. Lorber B, Berry M, Logan A, Tonge D (2002) Effect of lens lesion on neurite outgrowth of retinal ganglion cells in vitro. *Mol Cell Neurosci* 21:301–311
36. Fischer D, Petkova V, Thanos S, Benowitz LI (2004) Switching mature retinal ganglion cells to a robust growth state in vivo: gene expression and synergy with RhoA inactivation. *J Neurosci* 24:8726–8740
37. Lorber B, Berry M, Logan A (2005) Lens injury stimulates adult mouse retinal ganglion cell axon regeneration via both macrophage- and lens-derived factors. *Eur J Neurosci* 21:2029–2034
38. Liedtke T, Naskar R, Eisenacher M, Thanos S (2007) Transformation of adult retina from the regenerative to the axonogenesis state activates specific genes in various subsets of neurons and glial cells. *Glia* 55:189–201
39. Lorber B, Berry M, Logan A (2008) Different factors promote axonal regeneration of adult rat retinal ganglion cells after lens injury and intravitreal peripheral nerve grafting. *J Neurosci Res* 86:894–903
40. Heiduschka P, Thanos S (2006) Cortisol promotes survival and regeneration of axotomized retinal ganglion cells and enhances effects of aurintricarboxylic acid. *Graefes Arch Clin Exp Ophthalmol* 244:1512–1521
41. Muller A, Hauk TG, Fischer D (2007) Astrocyte-derived CNTF switches mature RGCs to a regenerative state following inflammatory stimulation. *Brain* 130:3308–3320
42. Berry M, Ahmed Z, Lorber B, Douglas M, Logan A (2008) Regeneration of axons in the visual system. *Restor Neurol Neurosci* 26:147–174
43. Chen L, Yang P, Kijlstra A (2002) Distribution, markers, and functions of retinal microglia. *Ocul Immunol Inflamm* 10:27–39
44. Moore S, Thanos S (1996) The concept of microglia in relation to central nervous system disease and regeneration. *Prog Neurobiol* 48:441–460
45. Sobrado-Calvo P, Vidal-Sanz M, Villegas-Perez MP (2007) Rat retinal microglial cells under normal conditions, after optic nerve section, and after optic nerve section and intravitreal injection of trophic factors or macrophage inhibitory factor. *J Comp Neurol* 501:866–878
46. Brinks H, Conrad S, Vogt J, Oldekamp J, Sierra A, Deitinghoff L, Bechmann I, Alvarez-Bolado G, Heimrich B, Monnier PP, Mueller BK, Skutella T (2004) The repulsive guidance molecule RGMA is involved in the formation of afferent connections in the dentate gyrus. *J Neurosci* 24:3862–3869
47. Yamashita T, Mueller BK, Hata K (2007) Neogenin and repulsive guidance molecule signaling in the central nervous system. *Curr Opin Neurobiol* 17:29–34
48. Lin L, Goldberg YP, Ganz T (2005) Competitive regulation of hepcidin mRNA by soluble and cell-associated hemojuvelin. *Blood* 106:2884–2889
49. Kuninger D, Kuns-Hashimoto R, Kuzmickas R, Rotwein P (2006) Complex biosynthesis of the muscle-enriched iron regulator RGMc. *J Cell Sci* 119:3273–3283
50. Kuninger D, Kuns-Hashimoto R, Nili M, Rotwein P (2008) Pro-protein convertases control the maturation and processing of the iron-regulatory protein. RGMc/hemojuvelin. *BMC Biochem* 9:9
51. Tassew NG, Charish J, Chestopalova L, Monnier PP (2009) Sustained in vivo inhibition of protein domains using single-chain Fv recombinant antibodies and its application to dissect RGMa activity on axonal outgrowth. *J Neurosci* 29:1126–1131
52. Kuns-Hashimoto R, Kuninger D, Nili M, Rotwein P (2008) Selective binding of RGMc/hemojuvelin, a key protein in systemic iron metabolism, to BMP-2 and neogenin. *Am J Physiol Cell Physiol* 294:C994–C1003
53. Tassew NG, Chestopalova L, Beecroft R, Matsunaga E, Teng H, Chedotal A, Monnier PP (2008) Intraretinal RGMa is involved in retino-tectal mapping. *Mol Cell Neurosci* 37:761–769
54. Matsunaga E, Chedotal A (2004) Repulsive guidance molecule/neogenin: a novel ligand-receptor system playing multiple roles in neural development. *Dev Growth Differ* 46:481–486
55. Matsunaga E, Nakamura H, Chedotal A (2006) Repulsive guidance molecule plays multiple roles in neuronal differentiation and axon guidance. *J Neurosci* 26:6082–6088
56. Conrad S, Genth H, Hofmann F, Just I, Skutella T (2007) Neogenin-RGMa signaling at the growth cone is bone morphogenetic protein-independent and involves RhoA, ROCK, and PKC. *J Biol Chem* 282:16423–16433
57. Mueller BK, Mueller R, Schoemaker H (2009) Stimulating neuroregeneration as a therapeutic drug approach for traumatic brain injury. *Br J Pharmacol* 157:675–685
58. Gonzenbach RR, Schwab ME (2008) Disinhibition of neurite growth to repair the injured adult CNS: focusing on Nogo. *Cell Mol Life Sci* 65:161–176
59. Guzik-Kornacka AM, Pernet VE, Joly SM, Martin JL, Schwab ME (2010) Role of neuronal Nogo-A in retinal axon regrowth after optic nerve injury. *Neuroscience 2010*. San Diego, CA, USA. Program Number 235.5; Poster Number D12
60. Meyerhardt JA, Look AT, Bigner SH, Fearon ER (1997) Identification and characterization of neogenin, a DCC-related gene. *Oncogene* 14:1129–1136
61. De Vries M, Cooper HM (2008) Emerging roles for neogenin and its ligands in CNS development. *J Neurochem* 106(4):1483–1492
62. Chauhan BK, Reed NA, Yang Y, Cermak L, Reneker L, Duncan MK, Cvekl A (2002) A comparative cDNA microarray analysis reveals a spectrum of genes regulated by Pax6 in mouse lens. *Genes Cells* 7:1267–1283
63. Grindley JC, Davidson DR, Hill RE (1995) The role of Pax-6 in eye and nasal development. *Development* 121:1433–1442